Simulation of Tissue Atrophy Using a Topology Preserving Transformation Model

Bilge Karaçali* , *Member, IEEE*, and Christos Davatzikos, *Member, IEEE*

***Abstract*—We propose a method to simulate atrophy and other similar volumetric change effects on medical images. Given a desired level of atrophy, we find a dense warping deformation that produces the corresponding levels of volumetric loss on the labeled tissue using an energy minimization strategy. Simulated results on a real brain image indicate that the method generates realistic images of tissue loss. The method does not make assumptions regarding the mechanics of tissue deformation, and provides a framework where a pre-specified pattern of atrophy can readily be simulated. Furthermore, it provides exact correspondences between images prior and posterior to the atrophy that can be used to evaluate provisional image registration and atrophy quantification algorithms.**

I. Introduction

COMPUTATIONAL anatomy schemes in medical image analysis rely on precise alignment of patient scans with a stereotactic atlas by deformation fields to quantify the morphology of anatomical structures. By comparing and contrasting volumetric measurements between different groups obtained from such deformation fields, morphological elements that characterize the attributes of respective groups can be identified [4], [2]. In the analysis of Alzheimer's disease, for instance, patterns of brain tissue loss in connection with abnormal aging are determined by examining the differences in the rates of longitudinal atrophy between a group of healthy seniors and a group of patients suffering from the Alzheimer's disease [3]–[5].

Despite their highly acclaimed status, these methods suffer from the lack of experimental validation. Establishing the accuracy and sensitivity of these methods requires ground truth data which is not available: given a set of medical images, volumes of specific regions of interest can be measured using computational methods, but without knowing the exact volumes of these anatomical structures, the reliability of measurements cannot be determined.

The lack of validation data poses a problem in evaluating the image registration algorithms upon which these schemes are based as well. Much work has been done in developing reliable and robust registration algorithms for intra-patient inter-modality, and inter-patient intra-modality registration, as well as other instances where correspondences between images of different nature are needed [6]. A satisfactory evaluation of registration accuracy, however, requires ground truth datasets, where exact dense correspondences between two subject images are known globally.

One method of generating ground truth datasets of volumetric change is to simulate tissue atrophy or growth in structural images. A straightforward simulation of volumetric change is by image magnification, as used by Freeborough and Fox [7]. The image of a structure of interest after magnification emulates local volumetric expansion, which is then used to validate an algorithm that quantifies rates of local volumetric change. Alternative approaches to simulate volumetric changes in tissues include those that employ operators from mathematical morphology, and biomechanical modeling using finite element methods. Mathematical morphology supplies operators such as dilation, erosion, closing and opening, that help reshape a given structure once it is identified in an image. The operators, when applied in specific ways, create desired changes in the shape and adjust the labels around the object boundaries as object or background. Müller and Rüegsegger [8] simulate trabecular bone atrophy by filtering a digital image of the bone by a Gaussian filter, and generating a binary image of an atrophied bone by thresholding the resulting grayscale image. They then find correspondences between the two by warping a finite element mesh to match the surfaces. The correspondences obtained by this algorithm between the original and the atrophied images, however, are bare estimates, and fall short of being ground truth correspondences.

Chen and Tsai [9] generate biological growth by first computing the stress distribution over a three dimensional structure using a finite element model, and use a growth law to calculate strains at each node. Davatzikos *et al.* [2] induce local atrophy to a select group of cortical structures using biomechanical deformations, and use the generated dataset to test the performance of an atrophy detection algorithm. Smith *et al.* [10] model the whole brain using a finite element structure, and use biomechanical deformations driven by specific thermal loads over the brain and the cerebrospinal fluid to induce global atrophy to select tissue types. An atrophied image is produced along with a finite-element deformation that links it to the original brain, that are then used to test the accuracy of a previously proposed method to measure atrophy.

In this paper, we propose an algorithm to simulate tissue atrophy on magnetic resonance (MR) images of a human brain through a topology-preserving deformation field that produces a given set of volumetric changes. Since the topology of the brain is not altered, the image after the atrophy can be used

Manuscript received October 27, 2005; revised February 16, 2006. This work was supported in part by the National Institutes of Health (NIH) under Grant R01 AG 14971 and ContractAG-93-07. *Asterisk indicates corresponding author.*

*B. Karaçali is with the School of Biomedical Engineering, Science, and Health Systems, Drexel University, 3120–24 Market Street, Philadelphia, PA 19104 USA (bilge@drexel.edu).

C. Davatzikos is with the Department of Radiology, University of Pennsylvania, Philadelphia, PA 19104 USA (christos@rad.upenn.edu).

Digital Object Identifier 10.1109/TMI.2006.873221

to evaluate the methods of computational anatomy that aim to quantify tissue loss. Furthermore, the images before and after the atrophy can be used to validate prospective image registration algorithms, since the deformation field that generates the atrophy also defines the exact point correspondences between the two images. The proposed method is automated, easily generalizable to other instances of spatially varying volumetric change, and can readily be modified to incorporate *a priori* knowledge in the form of a statistical atlas of tissue loss. Furthermore, the technique does not involve making any assumptions on how tissues deform, and produces visually realistic results.

We describe our approach to find a deformation field that produces a given set of volumetric effects in the next section. In Section III, we provide an empirical analysis of the algorithm on a real MR image of a human brain.

II. Approach

Atrophy in brain is characterized by tissue loss in either the gray matter (GM) or the white matter (WM), or simultaneously in both, typically due to aging or the progression of some medical condition. It can be regional or global with varying degrees over different regions. Ultimately, a significant loss in tissue volume is observed as the brain-cerebrospinal fluid boundary retreats, and the vacant space is occupied by the cerebrospinal fluid (CSF).

Our premise in this work is that tissue atrophy, as observed in the brain, can be characterized by a warping transformation that defines correspondences between the brain morphology prior and posterior to the atrophy. Given such a warping transformation, the exact pattern and amount of tissue loss can be identified and measured with high precision.

In simulating brain tissue atrophy, we seek a deformation that produces an array of desired volumetric changes, and specifically, volumetric loss. Given a set of volumetric changes we expect the brain to undergo in the course of atrophy, we aim to find a warping transformation that produces the prescribed effects. In order to make the simulation realistic, we introduce the following considerations: Firstly, the warping transformation of the atrophy should be obtained with no volumetric restrictions over the cerebrospinal fluid, since in actuality, the cerebrospinal fluid simply fills the void left by retreating tissue. This translates into letting the brain-cerebrospinal fluid boundary move freely through the simulation. In addition, the deformation over the skull should be zero since it does not get affected by the atrophy of the brain tissue. Finally, we also would like to constrain the solution to within a class of deformations for which topology is preserved.

A. Algorithm

Consider a brain image I defined a discrete regular grid $\Omega \subset \mathbb{R}^3$. Let $h : \Omega \rightarrow \mathbb{R}^3$ denote a warping transformation that deforms the image I into a new image I_d such that

$$I_d\left(h(\omega)\right) = I(\omega), \qquad \forall \omega \in \Omega. \tag{1}$$

Had h been defined over a continuum in $\mathbb{R}^3$, the volumetric change it induces onto I at a point ω could have been calculated by the determinant of its Jacobian matrix at ω. Since Ω is discrete, we compute the volumetric change h induces at ω by the average of corner Jacobians pertinent to ω. We have introduced corner Jacobians in the context of topology preserving regularity properties of dense discrete deformation fields [11], [12], and developed an algorithm to bound the corner Jacobians within a positive interval to satisfy the necessary conditions for topology preservation. Corner Jacobians represent the determinants of Jacobian matrices that correspond to forward and backward differences approximations to partial derivatives at a grid point ω. Since the partial derivatives along each Cartesian axis can be approximated in two ways, a total of eight different Jacobian determinants can be computed at a given point. For instance, the corner Jacobian that corresponds to forward differences approximations in x and y and backward differences approximation in z at $\omega = [x\ y\ z]^T$, $J_5(\omega)$, is defined by (2), shown at bottom of page. It can be shown that the average of these corner Jacobians is equivalent to the determinant of the Jacobian matrix constructed using the central differences approximations to the partial derivatives. Hence, the volumetric change induced by h at ω can be computed by the average of the corner Jacobians.

Suppose that a set of volumes $V(\omega)$ that specify the desired pattern of volumetric change over all $\omega \in \mathcal{B} \subset \Omega$ is given with $V(\omega) > 1$ indicating a volumetric increase, and $0 < V(\omega) < 1$ indicating atrophy with a percent rate of $100(1 - V(\omega))$. The set of grid points $\mathcal{B}$ denotes the region occupied by the brain. We propose to find a deformation field h that achieves the specified pattern of volumetric change by minimizing

$$H(h) = \frac{1}{2}\sum_{\omega\in\mathcal{B}}\left(\frac{1}{n(\omega)}\sum_{i=1}^{n(\omega)} J_i(\omega) - V(\omega)\right)^2 + \gamma\sum_{\omega\in\Omega}\sum_{i}\mathbf{1}_{(J_i(\omega)<\epsilon)}\left(\frac{J_i(\omega)}{\epsilon} + \frac{\epsilon}{J_i(\omega)} - 2\right) \tag{3}$$

where $n(\omega)$ denotes the number of available corner Jacobians $J_i(\omega)$ at ω enumerated by the index i, $0 < \epsilon < 1$, and γ is a weighting coefficient. The first term penalizes the deviation of the achieved rates of volumetric changes from those prescribed by $V(\omega)$. The second term prevents violation of topology

$$J_5(\omega) = \begin{vmatrix} f_{(x+1,y,z)} - f_{(x,y,z)} & f_{(x,y+1,z)} - f_{(x,y,z)} & f_{(x,y,z)} - f_{(x,y,z-1)} \\ g_{(x+1,y,z)} - g_{(x,y,z)} & g_{(x,y+1,z)} - g_{(x,y,z)} & g_{(x,y,z)} - g_{(x,y,z-1)} \\ e_{(x+1,y,z)} - e_{(x,y,z)} & e_{(x,y+1,z)} - e_{(x,y,z)} & e_{(x,y,z)} - e_{(x,y,z-1)} \end{vmatrix} \tag{2}$$

preservation conditions which require that all corner Jacobians be positive [12]. Using the chain rule of differentiation in (3) to compute the partial derivative of H with respect to $f(\omega_0)$, $\omega_0 \in \Omega$

$$\frac{\partial H}{\partial f(\omega_0)} = \sum_{\omega\in\mathcal{B}} \left(\frac{1}{n(\omega)} \sum_{i=1}^{n(\omega)} J_i(\omega) - V(\omega) \right) \left(\sum_{i=1}^{n(\omega)} \frac{\partial J_i(\omega)}{\partial f(\omega_0)} \right) + \gamma \sum_{\omega\in\Omega} \sum_{i} \mathbf{1}_{(J_i(\omega)<\epsilon)} \left(\frac{1}{\epsilon} - \frac{\epsilon}{J_i^2(\omega)} \right) \left(\frac{\partial J_i(\omega)}{\partial f(\omega_0)} \right) \quad (4)$$

and similarly for $g(\omega_0)$ and $e(\omega_0)$. Since $\partial J_i(\omega_0)/\partial f(\omega_0)$ can be derived in closed form for all i, the gradient of H with respect to h with Cartesian components f, g, and e along x, y, and z axes can be computed analytically. We, therefore, adopt a gradient descent strategy to minimize $H(h)$ for a topology preserving deformation field that achieves the prescribed set of volumetric measurements $V(\omega)$ over the brain tissue and preserves the topology of the original image (C code is available by request). An atrophied image is generated by warping the original image with the obtained deformation field, where the intensities of the expanded cerebrospinal fluid inside the region of atrophy are adjusted linearly to match those in the original image in mean and standard deviation.

B. Extended Algorithm

The procedure described above solves for a topology preserving deformation field that achieves a set of volumetric changes specified over each image voxel through an optimization procedure. For most cases, the procedure is expected to provide a deformation that induces the specified expansion and atrophy rates to a reasonable accuracy. On the other hand, the optimization may be strained to attain particularly large atrophy rates: in order to replace the retreating brain tissue, the regions of the cerebrospinal fluid have to expand at great rates, and trouble the topology preservation conditions. In order to address such issues, we expand the basic procedure above to incorporate a coordinate resampling step to relieve the strain on the optimization when simulating extensive atrophy rates. The extended algorithm is as follows:

- given an image I and a set of target volumes $V(\omega), \omega \in \mathcal{B}$;
- initialize $h^{(0)}(\omega) = 0$, $V_{\text{acc}}^{(0)}(\omega) = 1$, for all $\omega \in \mathcal{B}$;
- for $\mathrm{k} = 1, \ldots, \mathrm{K}$, do
  - compute $V_{\text{acc}}^{(k)} = \mathcal{W}_{h^{(k-1)}}(V_{\text{acc}}^{(k-1)})$
  - compute the target volumes $V^{(k)}(\omega) = V(\omega) \cdot V_{\text{acc}}^{(k-1)}(\omega)$
  - compute $h^{(k)}$ by carrying out the volume matching optimization to achieve the target volumes $V^{(k)}$;
- return $h = h^{(K)} \circ h^{(K-1)} \circ \cdots \circ h^{(0)}$, and I_d such that $I_d(h(\omega)) = I(\omega)$.

The operation $\mathcal{W}_h(V)$ redistributes the tissue volumes in V onto the grid points using the warping transformation h in a mass preserving manner, so that the total volume is preserved. For a smooth redistribution, it upsamples h and V, and directs the elements of the upsampled V to grid points specified by the upsampled h. Note that this redistribution increases tissue concentration at regions where the Jacobian determinant is low and vice versa, so that $(\mathcal{W}_h(\mathbf{1}))(\nu) \simeq n(\omega)/(\sum_{i=1}^{n(\omega)} J_i(\omega))$ for $\nu \simeq h(\omega)$. Hence, at iteration k, a deformation field $h^{(k)}$ is sought so that the product of volumetric changes induced by $h^{(k-1)} \circ h^{(k-2)} \circ \cdots \circ h^{(0)}$ at ω and $h^{(k)}$ at $\nu \simeq (h^{(k-1)} \circ h^{(k-2)} \circ \cdots \circ h^{(0)})(\omega)$ equals $V(\omega)$. Consequently, the accuracy of the overall deformation field $h^{(k)} \circ h^{(k-1)} \circ \cdots \circ h^{(0)}$ in generating the desired volumetric changes increases at each iteration.

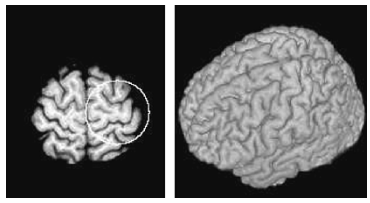

Fig. 1. The magnetic resonance image used in atrophy simulations.

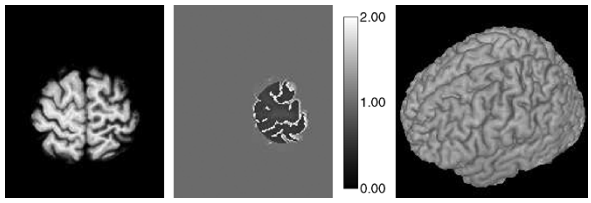

Fig. 2. Generated atrophy image using the basic algorithm at a target uniform atrophy level of 50% after 5000 iterations, with $\epsilon = 0.3$, together with the achieved rates of volumetric change. The average achieved atrophy is 33.74%.

III. Results

We have first evaluated the convergence properties of the basic algorithm that solves for a deformation field that achieves a given set of volumetric changes by minimizing (3). To this end, we have used a T1-weighted magnetic resonance images of a human brain, stripped the skull, removed the cerebellum, and resampled the remaining brain image in isotropic 1 mm^3 coordinates. Next, we have identified a region around the precentral gyrus over which we have simulated uniform atrophy at 10%, 20%, 30%, 40%, and 50%, by carrying out the iterations of the gradient descent scheme 200, 500, 1000, 2000, and 5000 times. The original image and the region of targeted uniform atrophy are shown in Fig. 1. The atrophy image obtained for a targeted atrophy of 50% after 5000 iterations along with the achieved volumetric change rates are shown in Fig. 2. The mean and standard deviations of the achieved volumetric changes within the region of targeted uniform atrophy for $\epsilon = 0.1, 0.2$, and 0.3 are shown in Table I. Not surprisingly, with more iterations, the algorithm is better able to achieve the targeted rate and with more homogeneity. However, it is also clear that large atrophy rates strain the algorithm and prevent convergence to the desired levels.

Next, we have used the extended algorithm to generate a 50% uniform atrophy in the same region. The results in Fig. 3 indicate that the introduced resampling strategy effectively relieves the strain on the basic algorithm, achieving the desired atrophy after $K = 7$ cycles and using only 200 iterations of the basic algorithm in each cycle. The simulation results at a target atrophy level of 70% in Fig. 4 make it evident that the extended algorithm can generate even larger rates of atrophy very precisely and in a topology preserving manner.

TABLE I
ACHIEVED ATROPHY RATES USING THE BASIC A LGORITHM FOR VARYING LEVELS OF TARGET ATROPHY AND VARYING NUMBER OF ITERATIONS. AVERAGE PERCENT ATROPHY AND STANDARD DEVIATION SHOWN

target	number of iterations				
rate	200	500	1000	2000	5000
$\epsilon = 0.1$					
10	8.63±1.42	9.49±0.64	9.79±0.29	9.89±0.17	9.89±0.14
20	12.50±5.04	14.36±4.50	15.15±4.17	15.97±3.75	16.84±3.16
30	14.76±8.01	17.12±7.82	18.68±7.55	19.91±7.25	21.64±6.68
40	16.90±10.51	19.14±10.56	21.04±10.47	22.85±10.28	25.40±9.82
50	17.03±12.40	19.67±12.78	21.90±12.93	24.45±12.92	27.80±12.68
$\epsilon = 0.2$					
10	9.03±1.09	9.56±0.56	9.76±0.32	9.90±0.14	9.95±0.06
20	12.95±4.92	14.84±4.29	15.93±3.76	16.84±3.20	17.86±2.37
30	16.06±7.89	18.39±7.55	20.22±7.11	21.73±6.60	23.53±5.79
40	17.41±10.45	20.33±10.38	22.77±10.14	25.09±9.75	28.02±8.97
50	19.07±12.50	22.24±12.67	25.11±12.62	27.64±12.43	31.46±11.86
$\epsilon = 0.3$					
10	9.03±1.09	9.59±0.52	9.79±0.28	9.92±0.10	9.98±0.02
20	13.46±4.76	15.37±4.03	16.47±3.42	17.46±2.72	18.47±1.80
30	16.81±7.73	19.35±7.25	21.16±6.73	22.79±6.09	24.87±4.97
40	17.24±10.26	21.36±10.10	24.23±9.72	26.64±9.21	29.85±8.15
50	18.25±12.11	23.17±12.33	26.53±12.21	29.61±11.87	33.74±11.00

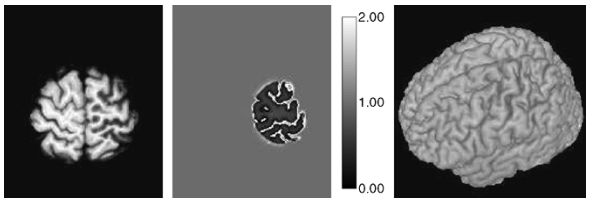

Fig. 3. Generated atrophy image using the extended algorithm at a targeted uniform atrophy level of 50%, using the basic algorithm at 200 iterations with $\epsilon = 0.2$ after $K = 7$ cycles, together with the achieved rates of volumetric change. The average achieved atrophy is 50.56% ± 17.03%.

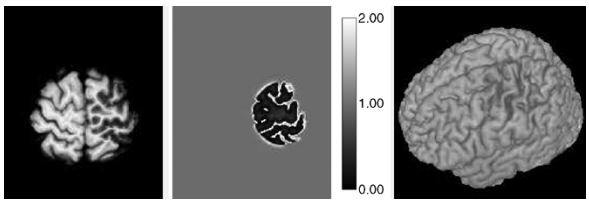

Fig. 4. Generated atrophy image using the extended algorithm at a targeted uniform atrophy level of 70%, using the basic algorithm at 200 iterations with $\epsilon = 0.2$ after $K = 9$ cycles, together with the achieved rates of volumetric change. The average achieved atrophy is 70.89% ± 17.10%.

IV. CONCLUSION

We have described an algorithm to compute a warping transformation, arguably one among a multitude of transformations depending on initialization, that produces a prescribed set of volumetric changes, and laid out the conditions according to which the algorithm is regulated in simulating brain tissue atrophy. These conditions include confinement to the space of inner skull, freely moving brain-CSF boundaries, and preservation of topology. The experimental results indicate that atrophy is simulated on real brain images using the proposed method with high fidelity realistic results.

The advantages of the proposed scheme include the simulation of visually realistic atrophy, the computational ease of the algorithm, and immunity to restrictive models and assumptions about the dynamics of tissue deformation. Indeed, any pattern of volumetric change can be induced on a given image to produce the desired effects. In cases where the volumetric change patterns in a clinical condition can be dictated by some *a priori* knowledge such as a statistical atlas, or if brain tissue material's response to missing mass could be modeled adequately, purely synthetic datasets can be generated faithful to the condition of interest. Computation of such an atlas of brain tissue loss due to aging, for instance, requires following a group of elderly individuals in time, and recording the levels of tissue loss measured in the coordinate system of a stereotactic atlas. Statistics can then be computed from these measurements, from which random but likely patterns of atrophy can be synthesized, increasing the reality of the simulation. Similarly, if the precise pattern of tissue loss is known, the algorithm can also be employed to "undo" the loss, and recover the morphology prior to the atrophy.

Another contribution of this work is that it provides a ground truth correspondence between the original image and the image after an induced volumetric change by means of a warping transformation. This correspondence is not only dense, it is also exact, in the sense that the generated image corresponds to the original image warped by the computed deformation field. In the future, the proposed algorithm will be used to generate such cases of ground truth data for the purpose of evaluating provisional image registration and atrophy quantization algorithms.

ACKNOWLEDGMENT

The authors thank the BLSA for providing the brain image.

REFERENCES

[1] S. L. Hartmann, M. Parks, H. Schlack, W. Riddle, R. R. Price, P. Martina, and B. M. Dawant, *Lecture Notes in Computer Science*, A. T.-P. Attila Kuba and M. Smal, Eds. Berlin, Germany: Springer-Verlag, 1999, vol. 1613, Automatic computation of brain andcerebellum volumes in normal subjects and chronic alcoholics, pp. 430–435.

[2] C. Davatzikos, A. Genc, D. Xu, and S. Resnick, "Voxel-based morphometry using the ravens maps: methods and validation using simulated longitudinal atrophy," *NeuroImage*, vol. 14, no. 6, pp. 1361–1369, 2001.

[3] N. C. Fox, R. I. Scahill, W. R. Crum, and M. N. Rossor, "Correlation between rates of brain atrophy and cognitive decline in ad," *Neurology*, vol. 52, pp. 1687–1689, 1999.

[4] C. Studholme, V. Cardenas, N. Schuff, H. Rosen, B. Miller, and M. W. Weiner, "Detecting spatially consistent structural differences in alzheimer's and frontotemporal dementia using deformation morphometry," in *Lecture Notes in Computer Science*, M. A. V. Wiro and J. Niessen, Eds. Berlin, Germany: Springer-Verlag, 2001, vol. 2208, MICCAI 2001, pp. 41–48.

[5] P. M. Thompson, K. M. Hayashi, G. de Zubicaray, A. L. Janke, S. E. Rose, J. Semple, D. Herman, M. S. Hong, S. S. Dittmer, D. M. Doddrell, and A. W. Toga, "Dynamics of gray matter loss in alzheimer's disease," *J. Neurosci.*, vol. 23, no. 3, pp. 994–1005, 2003.

[6] J. P. W. Pluim and J. M. Fitzpatrick, "Image registration," *IEEE Trans. Med. Imag.*, vol. 22, no. 11, pp. 1341–1343, Nov. 2003.

[7] P. Freeborough and N. Fox, "The boundary shift integral: an accurate and robust measure of cerebral volume changes from registered repeat MRI," *IEEE Trans. Med. Imag.*, vol. 16, no. 5, pp. 623–629, Oct. 1997.

[8] R. Müller and P. Rüegsegger, "Analysis of mechanical properties of cancellous bone under conditions of simulated atrophy," *J. Biomech.*, vol. 29, no. 8, pp. 1053–1060, 1996.

[9] J. L. Chen and W. C. Tsai, "Shape optimization by using simulated biological growth approaches," *AIAA J.*, vol. 31, no. 11, pp. 2143–2147, 1993.

[10] A. D. C. Smith, W. R. Crum, D. L. G. Hill, N. A. Thacker, and P. A. Bromiley, "Biomechanical simulation of atrophy in mr images," *Proc. SPIE*, vol. 5032, pp. 481–490, 2003.

[11] B. Karaçali and C. Davatzikos, "Topology preservation and regularity in estimated deformation fields," in *Lecture Notes in Computer Science*. Berlin, Germany: Springer-Verlag, 2003, vol. 2732, IPMI 2003, pp. 426–437.

[12] ——, "Estimating topology preserving and smooth displacement fields," *IEEE Trans. Med. Imag.*, vol. 23, no. 7, pp. 868–880, Jul. 2004.